Università degli Studi di Napoli Federico II

Facoltà di Medicina e Chirurgia

Dottorato di Ricerca in

Fisiopatologia Clinica e Medicina Sperimentale

(Coordinatore: Prof. Gianni Marone)

XXV Ciclo

Tesi di dottorato:

"miR-145 is a key regulator of the TGF-β signaling pathway in systemic sclerosis and counteracts experimental fibrosis"

Relatore:
Ch. mo Prof. Amato de Paulis

Candidata:
Dott. ssa Serena Vettori

Introduction

Systemic sclerosis (SSc) is a chronic, systemic fibrotic disorder of unknown origin that is characterized by microvascular abnormalitites, immune system activation, and progressive interstitial fibrosis in the skin and in target internal organs (heart, lungs, gastrointestinal tract, kidneys), that ultimately deranges tissue architecture and causes organ failure (1). Accordingly, SSc patients experience an increased morbidity and a premature mortality (2).

The turning point of fibrosis in SSc, as well as in other fibrotic disorders, independently from the triggering stimulus and the specific organ response, is the pathological activation of fibroblasts, which undergo an excessive synthesis and release of collagens and associated glycoproteins, and acquire a contractile phenotype due to the cytoplasmic accumulation of α-smooth muscle actin (α-SMA) (3). Soluble pro-fibrotic mediators, like Transforming Growth Factor (TGF)-β, Connective Tissue Growth Factor (CTGF), or Platelet-derived Growth Factor (PDGF) play a pivotal role in this process, as they mediate both the aberrant activation of fibroblasts and the persistence of this activated phenotype in an autocrine fashion (4). However, the mechanisms driving the escape of fibroblasts from connective tissue homeostasis are still unclear.

A new avenue of research to elucidate the regulation of the molecular players of fibrosis has been recently indicated by the study of microRNAs (miRNAs), a class of small (~ 22 nt), evolutionarily conserved, non-coding RNAs which binds to the 3' untranslated region (UTR) of target mRNAs, thereby inducing mRNA degradation or hampering translation (5). miRNAs have been associated to basic cellular processes, such as cell death, differentiation, and proliferation (6), and their dysregulation has been observed in various diseases, most notably cancers (7).

One of the most intriguing aspects of this regulatory machinery is that a single miRNA can simultaneously repress the expression of multiple genes, due to the partially complementary binding of a short recognition sequence (6 to 8 nt) of the miRNA to the 3' UTR of its target mRNAs (6).

This peculiar feature makes possible the regulation of a whole signaling pathway by a single miRNA acting at multiple levels, resulting in a robust down-regulation of the signal downstream (7). As a consequence, the aberrant expression of even a single miRNA can deeply change the physiologic response of a given cell type to external stimuli (7).

So far, few studies explored the function of miRNAs in SSc (8-11), and only two of them reached the level of target gene validation (8, 11). Hence, the purpose of our study was to search for dysregulated miRNAs in SSc that may have a significant functional impact on the pathophysiology of the disease by regulating key signaling pro-fibrotic pathways. This issue has never been addressed before.

Materials and methods

Patients, cell cultures, and mice

Skin specimens were obtained by punch biopsy from 12 SSc patients and 7 healthy controls (HC) from the distal aspect of one forearm after giving informed written consent. All patients fulfilled the ACR 1980 criteria for SSc (12), and underwent a complete clinical evaluation as summarized in table 1. One half of each sample was frozen in RNA later (Ambion/Applied Biosystems) and stored at -80° C or embedded in paraffin. The second half was used to expand skin fibroblasts by outgrowth culture in Dulbecco's modified Eagle's medium (DMEM), supplemented with 10% fetal calf serum (FCS), 2mM L-glutamine, 50U/ml penicillin/streptomycin, 0.2% Fungizone, and 10mM HEPES (all reagents provided by Gibco-Invitrogen) at 37°C 5% CO_2. Skin fibroblasts from passages 4-8 were used for the experiments. All human protocols were approved by the Review Board of the Zürich University Hospital.

DBA/2 mice were kindly provided by Dr. Jörg Distler's Laboratories, Institute for Clinical Immunology, University of Erlangen-Nuremberg, Germany. All mouse experiments were approved by the Government of Mittelfranken.

RNA isolation and microarray assay

Dermis from frozen skin biopsy specimens (0.5 cm^2) was separated from the epidermis with a scalpel using a stereofocal microscope, and homogenized with TissueLyser (Qiagen). A mirVana miRNA Isolation kit was used for isolation of total RNA (Ambion/Applied Biosystems) from both dermis and cultured cells. Two pools of 300 ng RNA from 3 SSc and 3 HC fibroblast samples (100 ng each) were used to screen the expression of 377 miRs by TaqMan Array Human MicroRNA Card A, in a 7900HT real-time polymerase chain reaction (PCR) system analyzer, according to manufacturer's instructions (all supplies provided by Applied Biosystems). Expression of the U6B

small nuclear RNA (RNU6B) was used as endogenous control to normalize the data. For relative quantification, the comparative threshold cycle (Ct) method was used (13).

Computational prediction analysis of miR-145 targets

Screening for miR-145 targets was performed by merging the results of several computational prediction algorithms provided at the miRGen database (http://www.diana.pcbi.upenn.edu/miRGen.html) (14). The miRGen database combines the results of computationally predicted target genes from optimized intersections and unions of the widely used mammalian target prediction programs PicTar, TargetScanS, miRanda, and DIANA-microT (15). These miRNAs are connected through the targets interface to their experimentally supported target genes from TarBase.

Transfection experiments

SSc and HC fibroblasts were transfected with a synthetic precursor (pre-miR-145) and an inhibitor of miR-145 (anti-miR-145), respectively, or with negative controls (Pre-miR/Anti-miRNegative Control #1; Ambion/Applied Biosystems) at a final concentration of 100 nM with the use of Lipofectamine 2000 reagent (Invitrogen), according to manufacturer's protocol. After 48 hours cell lysates were collected to analyze the expression of TGF-βII, TGF-βIII, TGF-βRII, Smad1, Smad3, CTGF, and types I and III collagen. Transfection efficiency was controlled by a TaqMan-based real-time PCR. At least 6 sets of cells were transfected for each group (SSc or HC).

Real time PCR analysis

For expression analysis of miRNAs, 10 ng of total RNA were reverse-transcribed using miR-143, miR-145, RNU6B, and Small nuclear (Sn)202 RNA specific stem-loop reverse transcription (RT) primers and the MicroRNA Reverse Transcription Kit (Applied Biosystems), according to the manufacturer's protocol. Real-time PCR was performed on 1 µl of the complementary DNA (cDNA) using specific FAM-labeled primers and TaqMan Universal PCR

Master Mix (Applied Biosystems) in a 7500 real-time PCR system (Applied Biosystems). Sn202 was used as endogenous control for mouse gene expression. For expression of pri-miR-143, pri-miR-145, human TGFB2, TGFB3, TGFBR2, SMAD1, SMAD3, CTGF, COL1A1, COL3A1, and mouse Tgfbr2, Smad3, and Col1a1 100 ng of total RNA were reverse-transcribed using random examers, Multiscribe reverse transcriptase 50 U/µl, RT buffer, dNTPs, and RNase inhibitor 20 U/µl (all Applied Biosystems). For pri-miR-143 and pri-miR 145 expression, specific TaqMan pre-developed assays were used (FAM, Applied Biosystems). Samples without the enzyme in the RT reaction were used as negative controls to exclude genomic contamination. The quality of the primer amplification was tested by dissociation curve analysis (15). To normalize for the amounts of loaded cDNA, a pre-developed 18S assay (PE Applied Biosystems) was used as an the endogenous control.

Western blot analysis

Cell lysates were prepared with Laemmli buffer. Equivalent amounts of protein from each samples were separated by sodium dodecyl sulfate–8% polyacrylamide gel electrophoresis and electrotransferred onto nitrocellulose membranes, as described previously (16). After blocking with 5% non-fat milk powder in TBS-T (0.05% Tween) for 1h, membranes were incubated overnight at 4°C with the following primary antibodies: polyclonal anti-human TGF-βRII (K105), monoclonal anti-human Smad3 (C67H9) (Cell Signaling Technology: 3713; 9520), polyclonal anti-human CTGF (H-55), polyclonal anti-human type I (H-70) and type III collagen (H-300) (Santa Cruz Biotechnology: sc-25440, sc-28655, sc-28888). After incubation with horseradish peroxidase (HRP)-conjugated goat anti-rabbit antibodies (Jackson ImmunoResearch) for 45 minutes, signals were detected with ECL (enhanced chemiluminescence) Western Blotting Detection Reagents (Amersham Bioscience) and exposure to x-ray film (Hyperfilm ECL, Amersham). For confirmation of equal loading of proteins, the amount of α-tubulin was determined, using mouse anti-human α-tubulin antibodies (Sigma) and HRP-conjugated goat anti-mouse antibodies (Jackson

ImmunoResearch). Semiquantitative analysis based on densitometry was performed using AlphaImager software (Alpha Imager).

Reporter gene assays

A 2254-bp fragment of the 3'UTR of TGFBR2, harbouring a conserved seed match for miR-145 at position 2194-2200, and three distinct fragments of the 3'UTR of SMAD3 of 1514 bp (SMAD3I), 1746 bp (SMAD3II), and 1465 bp (SMAD3III) respectively, harbouring two conserved seed matches for miR-145 at positions 1397-1404 (fragments I) and 3925-3931(fragment III) (informations provided by TargetScan database, release 5.2; http://www.targetscan.org), were amplified out of human genomic DNA. The PCR product for TGFBR2, SMAD3I, and SMAD3III were NheI digested, while the PCR product for SMAD3II was SalI digested. Each single fragment was cloned into the multiple restriction site of a pmirGLO Dual-Luciferase miRNA Target Expression Vector, downstream the stop codon of the Firefly luciferase gene (Promega). Mutant fragments of the both TGFBR2 and the three sequences of SMAD3 3'UTR, lacking the binding sites for miR-145, served as negative controls. The correct sequence and orientation of the inserts were confirmed by sequencing (Microsynth AG). Human Embrionic Kidney (HEK) 293 and Henrietta Lacks (HeLa) cells (5 x ^{10}cells/ml in 12-well plates) were co-transfected with 230 ng of either wild type or mutant constructs (pmirGLO-TGFBR2 3'UTR, pmirGLO-SMAD3I 3'UTR, pmirGLO-SMAD3II 3'UTR, and pmirGLO-SMAD3III 3'UTR) and 25 nM of pre-miR-145, using Lipofectamine2000 in antibiotic-free medium. Since a direct interaction of another miRNA, miR-20a, and the 3'UTR of TGFBR2 has been experimentally validated (predicted binding sites at positions 268-274 and 1201-1207), co-transfection of HEK 293 cells with the pmirGLO3'UTR of TGFBR2 construct and pre-miR20a served as the positive control. After 24h, Firefly luciferase activity was measured by the Dual-Luciferase Reporter Assay System (Promega), and normalized to the Renilla luciferase activity. At least 5 replicated for each co-transfection experiments were run.

Synthetic modified miR-145 design and animal experiments.

A synthetic analog of mature miR-145 (synth-miR-145) was designed for *in vivo* transfection of DBA/2 mice, as previously reported (17). Briefly, the miRNA sequence was methylated at position *2-O'* and phosphorotioate linkages were added at the flanking sites, and a cholesterol molecule was conjugated at the 3'end. A non-sense sequence (miR-scrambled control) of the same length of the mature miR-145 and carrying the same structural modifications was used as negative control. All synthetic miRNAs were purchased from Microsynth, Switzerland. Transfection efficiency without using any cationic lipid was tested *in vitro*.

Eighteen DBA/2 mice were used for the *in vivo* transfection experiments. Twelve mice underwent intradermal injection of bleomycin [0.5 mg/ml] in 100 µl NaCl in an area of 1.5 cm^2 of the upper back every other day for three weeks. Six of them were also injected with 3.75 nmol of synth-miR-145 in an equal volume of PBS every third day for all the three weeks (target group) of the bleomycin treatment, while 6 were injected with the scrambled control (synth-miR control group). Finally, the remaining 6 mice were injected with synth-miR-145 and NaCl using the same protocol (bleomycin control group). Mice were sacrificed by neck diversion two days after the last miRNA injection and the treated skin area was removed with a scalpel and put into RNA later for further RNA isolation.

Statistical analysis

GraphPad Prism 6.0 software was used for statistical analyses. Data were expressed as the mean ± SEM and median. Normal distribution of the data was tested using the Kolmogorov-Smirnov test, and student's unpaired t-test or Wilcoxon signed rank test were used as appropriate. P values less than 0.05 were considered statistically significant.

Results

miRNA expression profile of SSc fibroblasts and Real-time PCR confirmation of miR-145 down-regulation

Table 1 shows the low-density array analysis. Thirty-one out of 377 (8.2%) miRNAs were abnormally expressed in the pooled SSc fibroblasts as compared to the HC. Twenty-six out of 31 (83.9%) were found to be down-regulated, and 5/31 (16.1%) were found to be up-regulated. miR-145 was one of most down-regulated miRNAs with a nearly 90% reduction. This prompted us to run a real-time PCR for confirmation on 12 and 6 non-pooled SSc and HC fibroblasts, and on 11 SSc and 5 skin dermis samples, respectively. miR-145 expression was down-regulated by 45% in fibroblasts and by 50% in skin dermis ($p < 0.0001$ for both). Since miR-145 is clustered together with miR-143, we also looked for the expression of this miRNA in the same samples, but we found no difference between SSc and HC specimens.

Computational prediction analysis of miR-145 targets, target and collagens expression in transfected fibroblasts

Computational prediction analysis of miR-145 targets showed that TGFB2, TGFBR2, SMAD1, SMAD3, and CTGF were possible targets, as they were all predicted at least by two algorithms. Thus, we looked for the expression of these predicted targets in SSc fibroblasts over-expressing miR-145 (Table 3A) and in HC fibroblasts where miR-145 expression was inhibited (Table 3B) for confirmation. All the selected targets were modulated by miR-145 over-expression or inhibition. However, only TGFBR2, SMAD3, and CTGF show a statistically significant down-regulation in SSc fibroblasts transfected with pre-miR-145, by 50 to 60% ($p < 0.001$ for TGFBR2 and CTGF; $p < 0.01$ for SMAD3), as well as a significant up-regulation in HC fibroblasts transfected with anti-miR-145 ($p < 0.05$).

Since miRNAs are post-transcriptional regulators of gene expression, we also looked at changes in protein levels for all targets that were significantly regulated at the mRA level. As shown in figure 4, the down-regulation of both TGF-βRII and Smad3 in SSc fibroblasts transfected with pre-miR-145 was consistent with the real-time PCR findings.

Finally, to test whether the modulation of these components of the TGF-β signaling pathway and of the co-signaling molecule CTGF by miR-145 had really an impact on the production of collagens which are the final effectors of fibrosis, we looked at Collagens type I and type III expression in the same transfected cells. As shown in figure 5, both proteins were sign ificantly down-regulated. Similar results were obtained at the protein level.

Reporter gene assays and miR-145 target validation

The reported gene assay to show the direct interaction between miR-145 and the complementary binding site on TGFBR2 SMAD3 3'UTRs showed that both genes are targeted by miR-145, as predicted by the *in silico* analysis (figure 6). However, the co-transfection of HEK 293 cells with pre-miR-145 the pmiRGLO vector containing alternatively the 3'UTR of TGFBR2 and the three 3'UTR fragments of SMAD3, demonstrated a reduction of the Firefly versus the Renilla luciferase activity by more than 30% ($p < 0.01$). This effect was abolished in the cells co-transfected with the vector containing the mutated construct (figure 6A). On the contrary, the reduction of the Firefly versus the Renilla luciferase activity in HeLa cells co-transfected with the first (SMAD3I) and last (SMAD3III) fragments was lower than 80% and did not reach the statistical significance (figure 6B).

Animal experiments

The analysis of miR-145 expression in mice treated with synth-miR-145 showed that *in vivo* trasnfection was efficient, as miR-145 showed a 25 to 29 fold increased in injected animals, both treated with NaCl and bleomycin ($p = 0.004$; figure 7A). In addition, the analysis of the two major

miR-145 targets, showed a down-regulation from 60 to 80% of TGFBR2 and SMAD3 mRNAs ($p < 0.05$; figure 7B).

Conclusion

We found that miR-145 is down-regulated in human SSc dermal-derived fibroblasts and skin, and that this down-regulation accounts for the over-expression of at least two critical components of the TGF-β pathway, TGF-βRII and Smad3, and of the co-signaling molecule CTGF. Furthermore, and most importantly, here we show that miR-145 deficiency in a mouse model of skin sclerosis (bleomycin-induced skin sclerosis) can be corrected by the local administration of a synthetic modified miR-145, and that this treatment is effective in counteracting dermal fibrosis. Collectively, the data here presented indicate that miR-145 is a key player of fibrosis and traces the path for the development of a new potent therapeutic tool to be used in SSc and other fibrotic conditions.

Figure legend

Figure 1. The figure shows the expression profile of 31/377 miRNAs aberrantly expressed in pooled SSc and HC fibroblasts (n=3 each). A: down-regulated miRNAs. B: up-regulated miRNAs.

Figure 2. A: miR-145 down-regulation in SSc fibroblasts as analyzed by specific Real-Time PCR. B: expression of the same miRNA in skin dermis. For both analyses the p-value was < 0.0001.

Figure 3. Expression of the selected miR-145 predicted targets in SSc and HC controls fibroblasts (n=6 each group) transfected with pre- and anti-miR-145 respectively. All targets were found to be modulated by miR-145 over-expression/inhibition. *p-value < 0.05; **p-value < 0.01; ***p-value < 0.001.

Figure 4. TGF-βRII (A) and Smad3 (B) expression in SSc fibroblasts transfected with pre-miR-145 as evaluated by Western blot. Both ptoeins were down-regulated by 40%. *p-value < 0.05.

Figure 5. Collagen Type I (A) and type III (B) expression in SSc fibroblasts trasfected with pre-miR-145. The figure shows the down-regulation of both proteins by 45 (Collagen type I) and 35% (Collagen type III) respectively. *p-value < 0.05.

Figure 6. Reporter gene assay for TGFBR2 and SMAD3 3'UTRs. *p-value < 0.05.

Figure 7. A: miR-145 expression in animals treated with either synth-miR-145 or miR-scrambled. B: TGFBR2 and SMAD3 mRNA in mice treated bleomycin and either synth-miR-145 or miR-scrambled. ***p-value = 0.0004; *p-value < 0.05.

Table 1. Epidemiologic and clinical features of SSc patients enrolled in the study.

Patient	Age	Sex	Subset *	Abs	DD (RP)	DD (non-RP)	mRSS °	Organ involvement #	Biopsy §
1	27	F	lcSSc	ACA	5	3	4	Vascular, joint/tendon,upper GIT,lung	uninvolved
2	35	F	lcSSc (sine)	ANA	2	2	0	General,vascular, upper GIT	uninvolved
3	53	F	dcSSc	ANA	1	2	21	General,vascular, joint/tendon,upper GIT,lung, heart	involved
4	31	F	lcSSc	ACA	2	0	5	Vascular,upper GIT, lung	uninvolved
5	52	F	dcSSc	ANA	1.5	0.5	20	General,vascular, joint/tendon,muscle , upper GIT,lung	involved
6	55	M	lcSSc (sine)	Scl70	2	1	0	Vascular, upper GIT	uninvolved
7	24	M	lcSSc (sine)	ACA	2	2	0	Vascular, upper GIT, lung, heart	uninvolved
8	51	F	lcSSc	ACA	0.5	0.5	6	Vascular,upper GIT, lung	involved
9	48	F	lcSSc	ACA	32	15	6	Vascular, joint/tendon,upper GIT, lung	involved
10	38	F	dcSSc	Scl70	12	12	10	Vascular, joint/tendon,muscle , upper GIT,lung	involved
11	50	F	dcSSc	Scl70	3	6	16	Vascular,upper GIT, lung	involved
12	20	F	lcSSc	Scl70	13	0	1	General,vascular, upper GIT,lung	uninvolved

*Clinical subset was defined according to LeRoy and Medsger; °mRSS = modified Rodnan skin score; #organ involvement was evaluated according to EUSTAR assessment criteria; §biopsy site was the distal aspect of a forearm in all patients and the presence/absence of skin involvement at the time of the biospy is reported.

Ab = autoantibodies; DD = disease duration; RP = Raynaud's phenomenon; non-RP = 1st symptom correlated to SSc different from RP; lcSSc = limited cutaneous systemic sclerosis; dcSSc = diffuse cutaneous systemic sclerosis; sine =

sine scleroderma systemic sclerosis; ANA = anti-nuclear antibodies; ACA = anit-centromere antibodies; Scl70 = anti-Scl70 (anti-topoisomerase I) antibodies; GIT = gastrointestinal tract

Figure 1

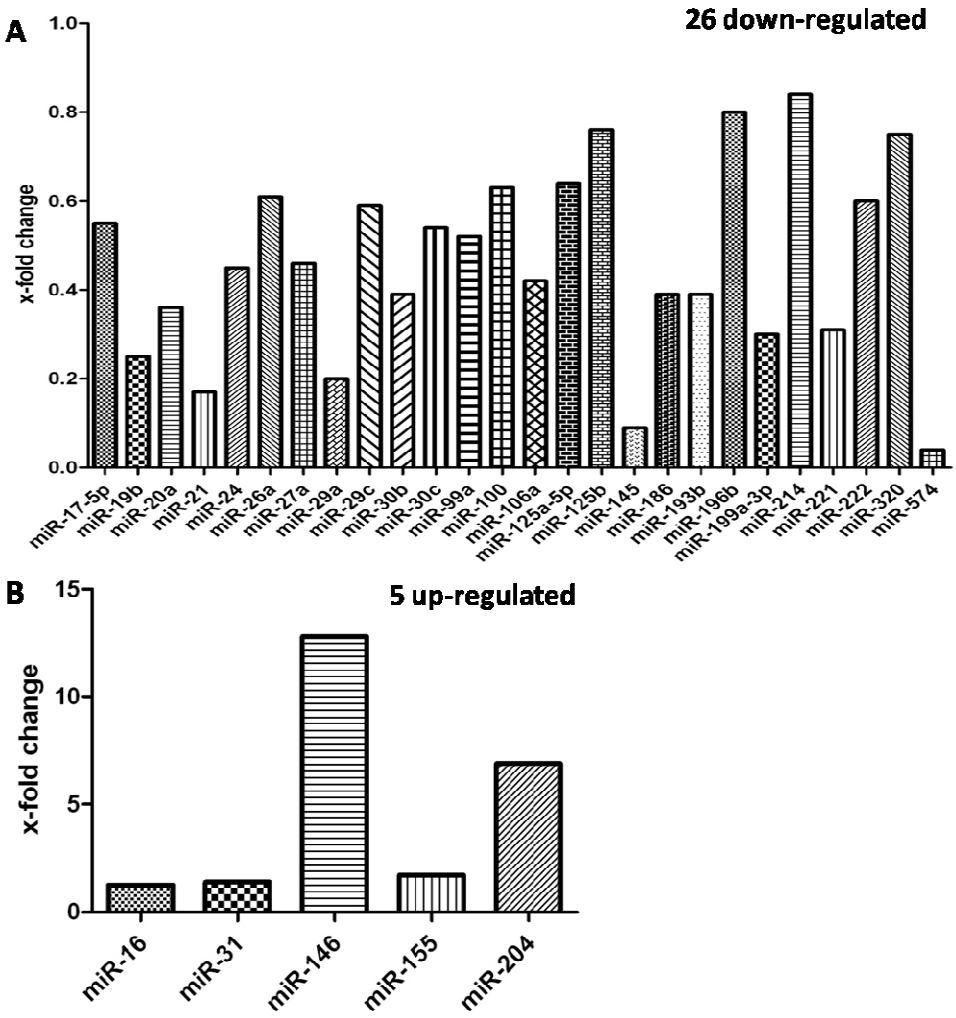
A
26 down-regulated
x-fold change
1.0
0.8
0.6
0.4
0.2
0.0
miR-17-5p
miR-19b
miR-20a
miR-21
miR-24
miR-26a
miR-27a
miR-29a
miR-29c
miR-30b
miR-30c
miR-99a
miR-100
miR-106a
miR-125a-5p
miR-125b
miR-145
miR-186
miR-193b
miR-196b
miR-199a-3p
miR-214
miR-221
miR-222
miR-320
miR-574
B
5 up-regulated
x-fold change
15
10
5
0
miR-16
miR-31
miR-146
miR-155
miR-204

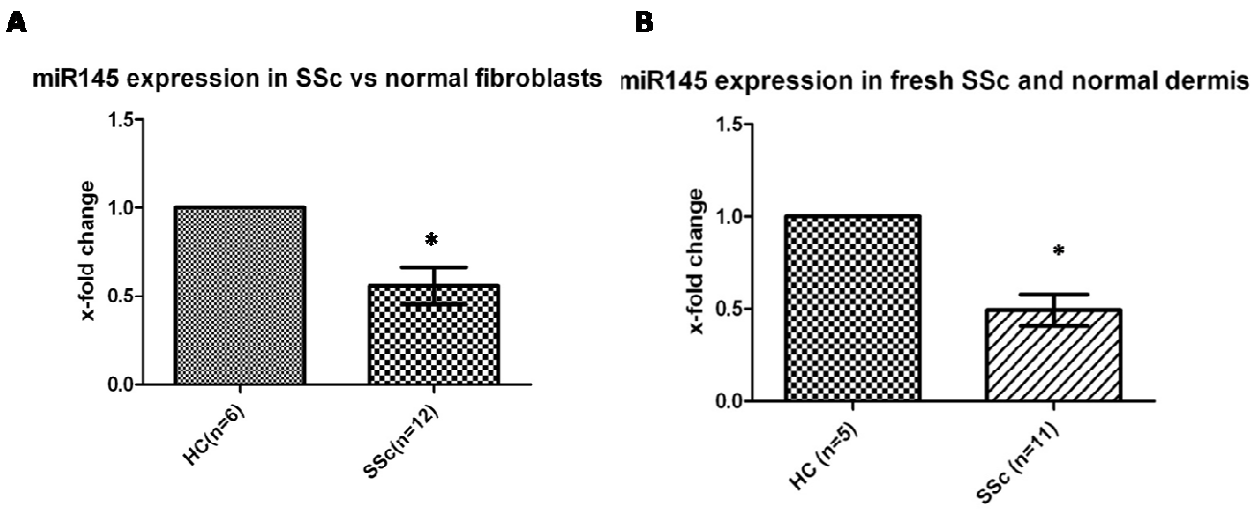
A
miR145 expression in SSc vs normal fibroblasts
x-fold change
1.5
1.0
0.5
0.0
*
HC(n=6)
SSc(n=12)
B
miR145 expression in fresh SSc and normal dermis
x-fold change
1.5
1.0
0.5
0.0
*
HC (n=5)
SSc (n=11)

Figure 2

Figure 3

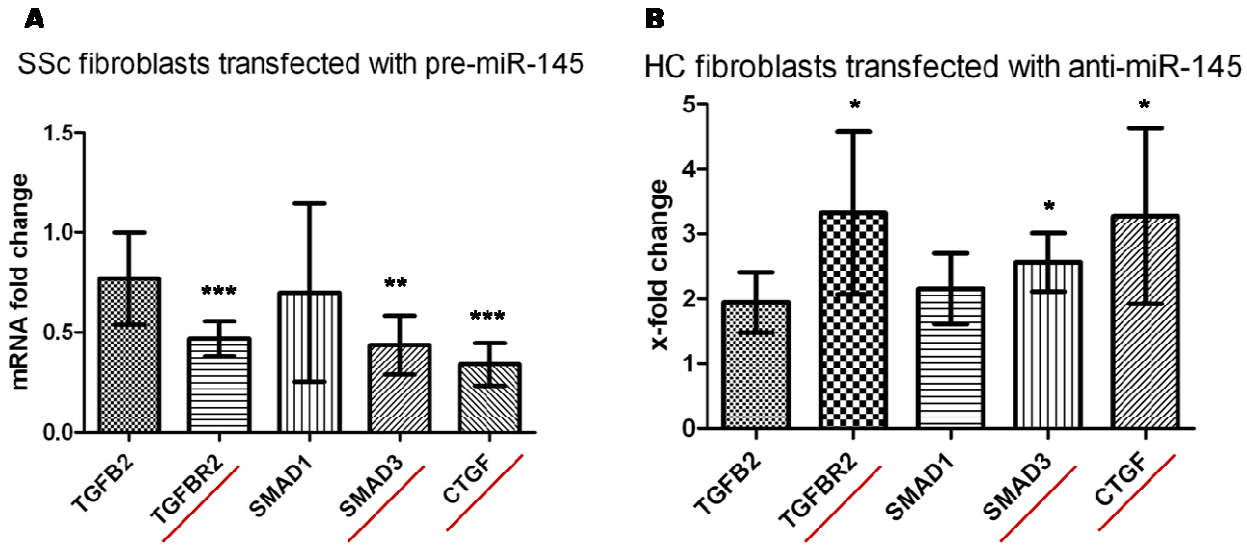
A
SSc fibroblasts transfected with pre-miR-145
mRNA fold change
1.5
1.0
0.5
0.0
***
**
***
TGFB2
TGFBR2
SMAD1
SMAD3
CTGF
B
HC fibroblasts transfected with anti-miR-145
x-fold change
5
4
3
2
1
0
*
*
*
TGFB2
TGFBR2
SMAD1
SMAD3
CTGF

Figure 4

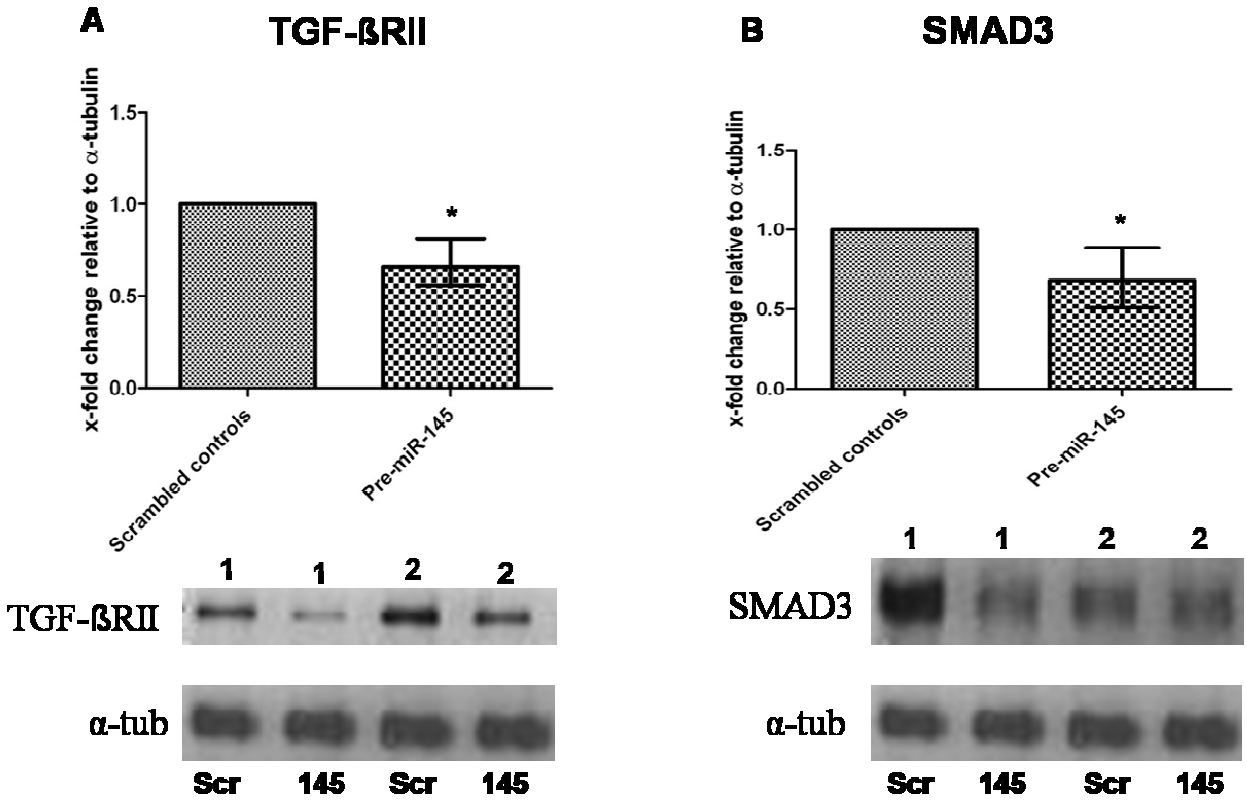
A
TGF-ßRII
x-fold change relative to α-tubulin
1.5
1.0
0.5
0.0
*
Scrambled controls
Pre-miR-145
1
1
2
2
TGF-ßRII
α-tub
Scr
145
Scr
145
B
SMAD3
x-fold change relative to α-tubulin
1.5
1.0
0.5
0.0
*
Scrambled controls
Pre-miR-145
1
1
2
2
SMAD3
α-tub
Scr
145
Scr
145

Figure 5

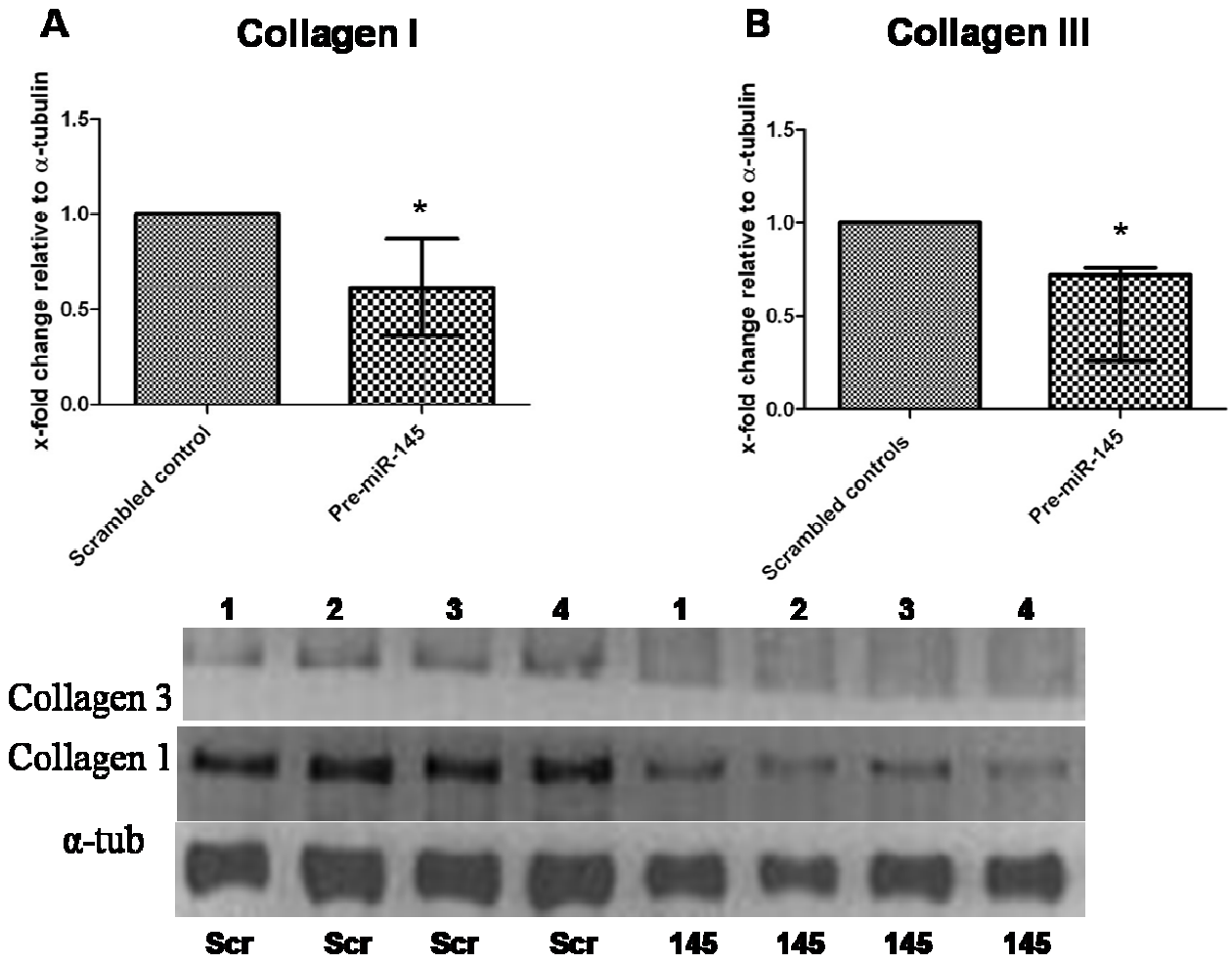
A
Collagen I
x-fold change relative to α-tubulin
1.5
1.0
0.5
0.0
*
Scrambled control
Pre-miR-145
B
Collagen III
x-fold change relative to α-tubulin
1.5
1.0
0.5
0.0
*
Scrambled controls
Pre-miR-145
1 2 3 4 1 2 3 4
Collagen 3
Collagen 1
α-tub
Scr Scr Scr Scr 145 145 145 145

Figure 6

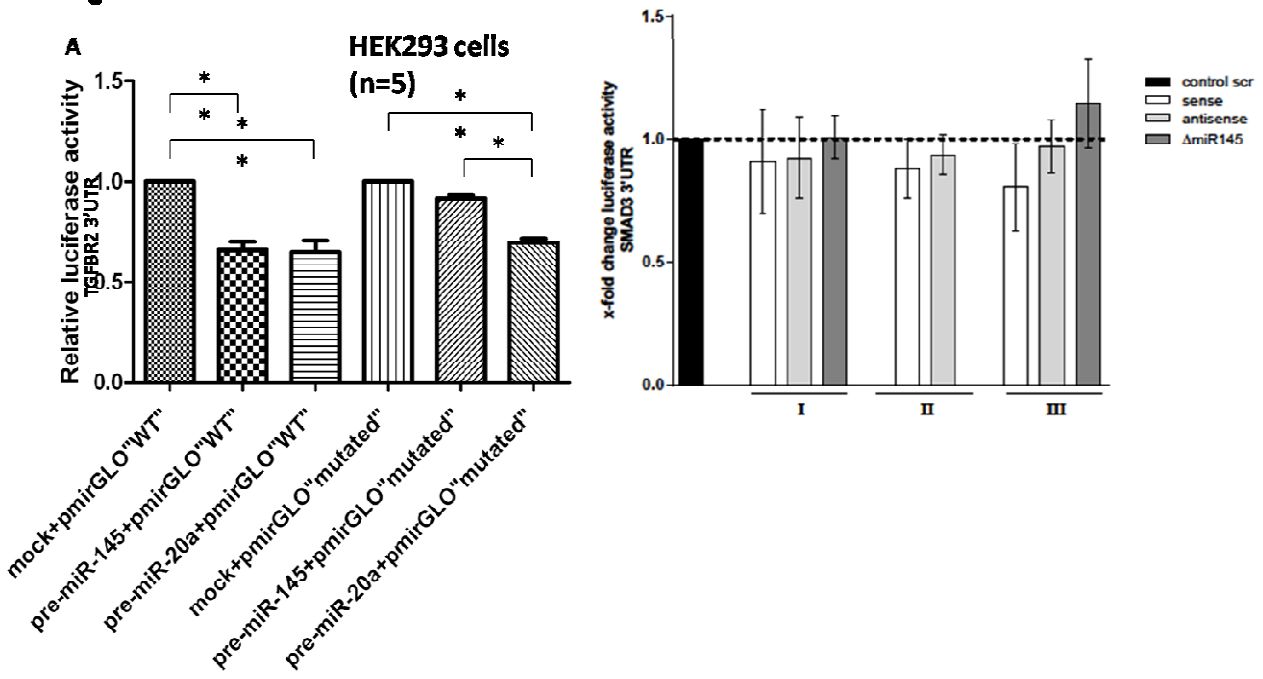
A
HEK293 cells
(n=5)
Relative luciferase activity
TGFBR2 3'UTR
1.5
1.0
0.5
0.0
mock+pmirGLO"WT"
pre-miR-145+pmirGLO"WT"
pre-miR-20a+pmirGLO"WT"
mock+pmirGLO"mutated"
pre-miR-145+pmirGLO"mutated"
pre-miR-20a+pmirGLO"mutated"
x-fold change luciferase activity
SMAD3 3'UTR
control scr
sense
antisense
ΔmiR145
I
II
III

Figure 7

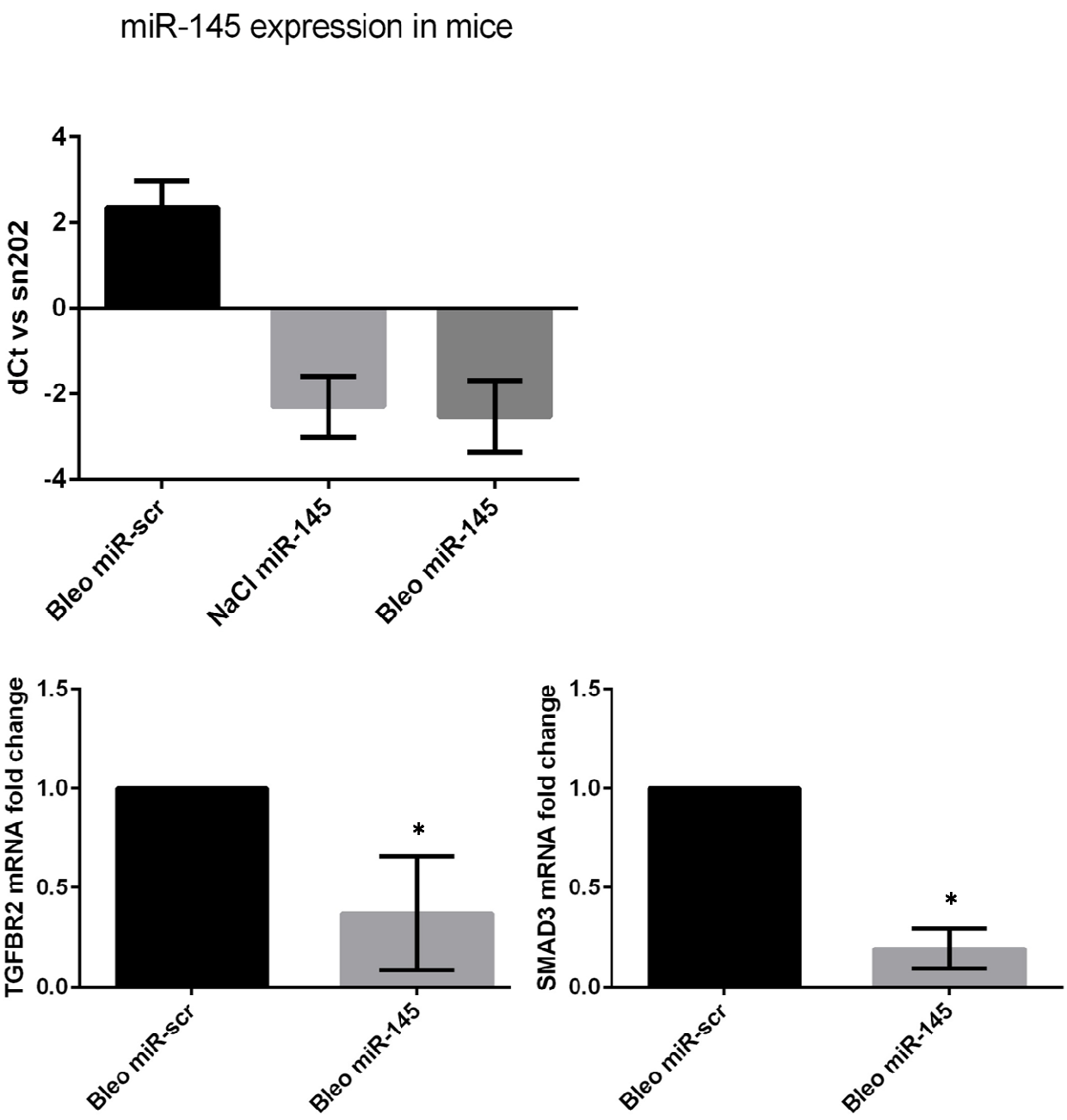
miR-145 expression in mice
dCt vs sn202
4
2
0
-2
-4
Bleo miR-scr
NaCl miR-145
Bleo miR-145
TGFBR2 mRNA fold change
1.5
1.0
0.5
0.0
*
Bleo miR-scr
Bleo miR-145
SMAD3 mRNA fold change
1.5
1.0
0.5
0.0
*
Bleo miR-scr
Bleo miR-145